Adaptive Filter Design for Simultaneous In-band Full-duplex Communication and Radar

Seyed Ali Hassani[†1], Barend van Liempd[# 2], André Bourdoux[# 3], François Horlin[*4] and Sofie Pollin[†# 5]

[†]Department of Electrical Engineering, KU Leuven, Belgium

[#]Imec, Leuven, Belgium

[*]Université Libre de Bruxelles, Belgium

{[1]seyedali.hassani, [5]sofie.pollin}@kuleuven.be, {[2]barend.vanliempd, [3]andre.bourdoux}@imec.be, [4]fhorlin@ulb.ac.be

***Abstract* — The in-band full-duplex (IBFD) wireless communication can achieve not only appreciable throughput gain but also is a key technology to enable concurrent radar and communication by one hardware. In such a system, an analog self-interference (SI) canceller is essential so that the received signal can be processed digitally to achieve sufficient SNR for IBFD communication. Unlike the previous similar works which rely on a classical matched filter, this paper derives the range-Doppler profile from the state of an adaptive filter, which primarily is applied to cancel the residual SI. Using standard IEEE 802.11ac signal, the proposed waveform-independent technique in this paper is simulated in a multi-target IBFD scenario. Furthermore, we employed a proof of concept setup to validate the proposed approach. The simulation and experimental results confirm that our method can render accurate range and velocity detection, and potentially satisfies a wide spectrum of opportunistic wireless sensing applications, ranging from hand/body gesture detection to tracking and localization.**

***Keywords* — in-band full-duplex, self-interference cancellation, mono-static radar, opportunistic wireless sensing, hand/body gesture detection, WiFi sensing.**

I. Introduction

Due to its remarkable features, wireless sensing technology has strong potentials in indoor and outdoor applications. The challenge is to implement such a functionality opportunistically and efficiently, without the need for extra hardware, power, or spectrum. Such an innovative radar capability integrated into a communication device is not yet standardized. However, due to the recent advances and the ease of deployment, it would not be surprising to become a part of the wireless networking standards in the near future.

There is a substantial body of literature that employs an already-existing communication signal to extract the Doppler information, often in a bi-static scheme. A bi-static Doppler radar relies on a matched filter, which reconstructs the Doppler out of the surveillance signal and the reference from the line-of-sight of the transmitter of opportunity. Various approaches have been proposed which remove the unwanted echoes affecting the signal received at the surveillance antenna. For instance, the use of directional antennas, and employing an adaptive filter [1]–[3] that actively removes the reference signal. In [4]–[6], the radar functionality is carried out by leveraging the channel estimation technique for a particular modulation, the orthogonal frequency-division multiplexing (OFDM) scheme, where the samples obtained at the output of the receiver are divided by the known transmitted data symbol to yield the discrete Fourier transform (DFT) of the channel coefficients.

Although the in-band full-duplex (IBFD) technology is well-known from the spectral efficiency point of view, it also offers promising solutions to address the existing gaps in opportunistic wireless sensing. The key technical challenge to realize concurrent in-band send and receive is to overcome the high-power self-interference (SI). Typically, IBFD transceivers somewhat suppress the SI signal before sampling, avoiding the analog-to-digital converter (ADC) saturation. This step enables further SI cancellation at the digital sampled baseband.

In [7] and [8], the authors introduce an IBFD communication architecture that also accomplishes Doppler sensing in a mono-static scheme. They developed and prototyped the system [9] in which an electrically balanced duplexer provides the prerequisite Tx-Rx isolation at RF. Then, a classical correlation-based radar is implemented to compute the Doppler state of the channel out of the environmental echoes of the self-transmit communication signal. Although the proposed scheme in their work allows joint in-band bi-directional messaging and Doppler radar via a single platform, a WiFi access point for example, it requires a trade-off between sensing and communication functionalities. The reason is behind the fact that the SI canceller modules have to remain unchanged during the period that the device performs Doppler detection. Otherwise, it also suppresses the echo from the target as it is highly correlated with the SI signal [9]. Thus, the system compromises the level of Tx-Rx isolation, which principally influences IBFD communication performance [8].

The proposed approach followed in this paper implements an adaptive filter which accomplishes both dynamic SI suppression and Doppler sensing, without compromising the performance of SI cancellation. Furthermore, our method allows for range detection and is waveform-independent, which makes it perfectly suitable for WiFi sensing applications and IBFD radar-communication systems, where multiple devices can collaborate to perform target tracking and user localization.

The rest of the paper is organized as follows. Sec. II formulates a mathematical model that describes the introduced approach. Sec. III represents the simulation, where the validity of the proposed technique is assessed through numerical

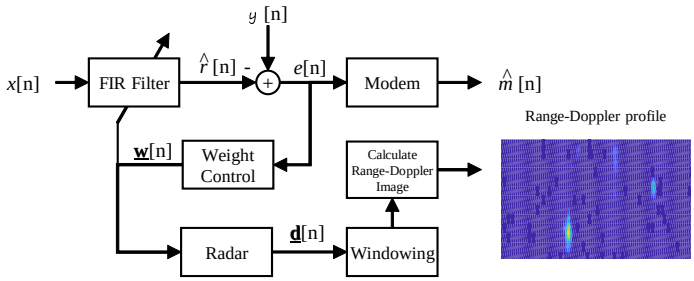

Fig. 1. Overview of the proposed radar-capable self-interference cancellation system. While the adaptive filter is seeking to minimize the self-interference signal, the computed filter coefficients are analyzed to determine the 2-D radar image.

analysis. Sec. IV includes the experimental result, and finally, the conclusion is drawn.

II. Mathematical Model for Joint Radar and Self-interference Cancellation

Fig. 1 depicts the overview of the proposed system, where an adaptively tuned digital filter is exploited to drive both communication modem and radar.

For clarity, the mathematical model will be developed for a noise-less system in the sampled baseband domain. By design, the sampling frequency f_s is assumed to be an integer (N) multiple of the communication bandwidth B.

To form an in-band bi-directional link, the model adopts two transceivers, labeled by **X** and **M**, which transmit the baseband communication signals $x[n]$ and $m[n]$, respectively. Let take **X** as the radar-enabled node, which receives the baseband signal $y[n]$ in the form

$$y[n] = r[n] + m_c[n], \tag{1}$$

where $r[n]$ is the SI signal, and $m_c[n]$ denotes the baseband representation of the message from **M**, which is influenced by the channel between the two devices.

Note that $r[n]$ consists of the residual direct Tx leakage after the analog SI suppression and the reflected self-transmit signal from the environment.

By employing the channel model in [10], we describe $r[n]$ in the form of time-delayed, phase-shifted and attenuated replicas of the communication signal $x[n]$, i.e.,

$$r[n] = \sum_{\rho} A_\rho e^{j(\mathcal{W}_\rho n + \phi_\rho)} x[n - \Delta_\rho], \text{ and } \Delta_\rho = \lfloor \frac{2 d_\rho f_s}{c} \rceil, \tag{2}$$

where A_ρ, ϕ_ρ and Δ_ρ denot, respectively, the attenuation, phase shift and delay of the ρ^{th} reflection path, d_ρ is the distance of the reflector, and c stands for the speed of the light. Besides, $\mathcal{W}_\rho$ denotes the Doppler frequency shift of the ρ^{th} reflector.

Note that the contributions from the static environment and the direct Tx leakage produce echoes with a zero-frequency Doppler shift.

A. Self-interference Cancellation

As shown in Fig. 1, to enable IBFD communication, the adaptive filter reconstructs the residual SI signal, resulting in the error signal $e[n]$, as defined in (3).

$$e[n] = y[n] - \hat{r}[n], \tag{3}$$

where $\hat{r}[n]$ denotes the estimate of the SI signal, synthesized by a finite impulse response (FIR) filter.

The output of the FIR filter is a linear combination of multiple time-delayed versions of the Tx signal in the form

$$\hat{r}[n] = \underline{\mathbf{w}}^*[n] \underline{\mathbf{x}}^{\mathrm{T}}[n], \tag{4}$$

where the vector $\underline{\mathbf{w}}[n] = [\mathrm{w}_0[n], \mathrm{w}_1[n], ..., \mathrm{w}_{Q-1}[n]]$ represents the coefficients of the FIR filter at the discrete-time n. Similarly, the reference vector $\underline{\mathbf{x}}[n] = [\mathrm{x}[n], \mathrm{x}[n-1], ..., \mathrm{x}[n-Q-1]]$ holds the Q most recent samples of the Tx signal $x[n]$, and the superscripts $^{\mathrm{T}}$ and * denote the matrix transpose and complex conjugate, respectively.

Various adaptation techniques have been proposed to update a FIR filter [11]. Due to its implementation simplicity and rapid convergence, our model makes use of the normalized least mean squares (NLMS) algorithm to update the coefficients as follows.

$$\underline{\mathbf{w}}[n+1] = \underline{\mathbf{w}}[n] + \frac{\mu e^*[n] \underline{\mathbf{x}}[n]}{\varepsilon + \underline{\mathbf{x}}[n] \underline{\mathbf{x}}^{\mathrm{H}}[n]}, \tag{5}$$

where ε is the regulation parameter which prevents large step sizes, μ is the fixed convergence parameter, and the superscript $^{\mathrm{H}}$ denotes the complex conjugate transpose.

Herein, we assume that the filter adaptation rate is the same as the baseband sample rate f_s. Note that given $x[n]$ and $m[n]$ are statistically independent, the error signal $e[n]$ in (3) converges to $m_c[n]$ [11], so that the modem can reconstruct the emitted communication message from **M**, shown by $\hat{m}[n]$ in the block diagram.

B. Range-Doppler Radar

In the radar point of view, the range resolution of such a system depends on the total bandwidth occupied by the communication signal $x[n]$, i.e.,

$$R_{res} = \frac{c}{2B}. \tag{6}$$

Let us define P_b as the set of reflectors located in the b^{th} radar range bin $R_b = [bR_{res}, (b+1)R_{res})$, from which the echoed SI signals reach the radar within nearly an identical delay Δ_b. Accordingly, one can approximate the SI signal in (2) as a sum of the reflections from the radar range bins, as follows.

$$r[n] \approx \sum_{b} \alpha_b[n] x[n - \Delta_b], \tag{7}$$

where $\alpha_b[n]$ characterizes the reflected SI components from the b^{th} range bin by their amplitude and phase/frequency shift, i.e.,

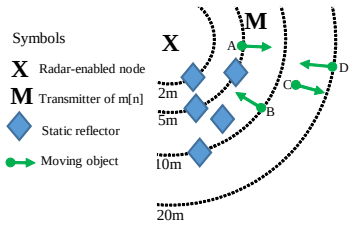

Fig. 2. Simulation layout, including two communication devices, static scatters, and dynamic objects shown by A, B, C and D, moving at the speed of -2.5, 5, -7.5 and 10 m/s, respectively.

$$\alpha_b[n] = \sum_{\rho \in P_b} A_\rho e^{j(\mathcal{W}_\rho n + \phi_\rho)}. \tag{8}$$

Given the system acquires $N = f_s/B$ samples within the coherence time of the communication signal $x[n]$, from (4) and (7), one can estimate the cellwise Doppler information in (8) through N successive coefficients of the adaptive filter as follows.

$$\hat{\alpha}_b[n] = \sum_{k=0}^{N-1} \mathrm{w}_{Nb+k}[n] \tag{9}$$

To only sense the nonstationary objects, the system employs a DC-removal filter that rejects the zero-frequency Dopplers. Further, the sample rate of the communication signal is multiple times larger than the maximum Doppler frequency shift in the intended applications by this paper. Thus, decimation is required to form a narrowband Doppler signal and filter out any abrupt variation. Consequently, we use low-pass filtering and downsampling to reconstruct the non-zero Doppler information of the b^{th} range bin as

$$d_b[n] = (h[n] * \hat{\alpha}_b[n])_{\downarrow N_d}, \tag{10}$$

where $h[n]$ denotes the band-pass filter, combining the DC-removal and the low-pass filter described above, $(*)$ stands for the time-domain convolution, and the operation $\{.\}_{\downarrow N_d}$ is the downsampling by a factor of N_d.

Next, the radar range-Doppler profile resulting from the proposed approach can be defined in the form

$$\underline{\mathbf{d}}[n] = [d_0[n], d_1[n], ..., d_{\frac{Q}{N}-1}[n]], \tag{11}$$

where the b^{th} element of $\underline{\mathbf{d}}[n]$ approximates the Doppler information reflecting off the range bin R_b.

Finally, the fast Fourier transform (FFT) can be used to identify the dominant Doppler component of each range bin $\mathcal{W}_d$, and consequently, calculate the radial speed of the target V, the velocity resolution V_{res} and the maximum detectable speed V_{max} as follows.

$$V = \frac{c\mathcal{W}_d}{4\pi f_c}\ ,\ V_{res} = \frac{cf_s}{2f_c N_d N_{fft}},\ V_{max} = \frac{cf_s}{4f_c N_d}, \tag{12}$$

Table 1. IEEE 802.11ac OFDM Waveform Characteristics

Conf.	Value	Conf.	Value
strength	27 dBm	Num. PSDU Packets	500
band	5 GHz	OFDM subcarriers	242 (Data+Pilot)
bandwidth	80 MHz	modulation	64 QAM (5/6)
ideal time	20 μs	PHY data rate	325 Mbps

where N_{fft} stands for the number of samples used to produce the FFT and f_c is the carrier frequency of the communication signal.

Besides, the filter order Q and the processing gain N determine the maximum detectable range, i.e.,

$$R_{max} = \frac{QR_{res}}{N}. \tag{13}$$

III. Simulation

To evaluate the proposed system, a numerical model is implemented in Matlab™, in which different signals are generated to resemble a multi-target radar scenario, as illustrated in Fig. 2. As shown, five static reflectors and four moving objects, with radar cross-section factor of 8 $dBsm$, are located at different distances relative to the IBFD radar-capable device. The two IBFD transceivers, represented by **X** and **M** in the simulated layout, produce standard IEEE 802.11ac waveform with the parameters specified in Table 1 from random and zero-mean binary information. The generated 80 MHz baseband communication signals are sampled at 160 MHz ($N = 2$) while there is a 20 μs interval between each two successive physical layer service data unit (PSDU) packets. For each of the static and dynamic reflectors, the time delay, phase/frequency shift, and attenuation are computed individually. We also applied 50 dB SI suppression for the direct Tx leakage.

Then, the signal components resulting from the different scatters, direct Tx leakage, the emitted signal from **M**, and the thermal noise (-90 dBm) are superimposed, resulting in the baseband received signal $y[n]$ as defined in (1). A 28-tap adaptive filter is also implemented that makes use of a NLMS optimizer to achieve > 35 dB additional SI rejection within $T_c = 1.3$ ms convergence time. This enables sufficient Tx-Rx isolation, which is required for in-band bi-directional communication. The weight vector of the adaptive filter is then served to estimate the Doppler information of each range bin as described in (8)-(11). The resultant signal is also decimated ($N_d = 2^{17}$) and DC-removed. We employed a Hanning window and FFT to estimate the power intensity. Fig. 3 represents the 2-D range-Doppler image produced from 600 PSDU packets transmitted within 100 ms. Assuming the carrier at 5 GHz frequency band, the described configuration allows sensing of objects up to $R_{max} = 24.32$ m away from the radar, moving below $V_{max} = 27.44$ m/s, and the range and speed resolution of 1.87 m and 0.3 m/s, respectively (see (12) and (13)). The graph in Fig. 3 proves that the proposed approach can estimate the relative distance and speed of the targets, bounded by the theoretical limits.

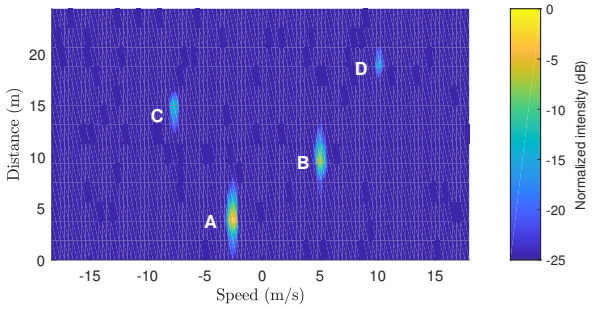

Fig. 3. Simulation result: computed range-Doppler profile, resulted from applying the proposed processing approach to the weight vector of the adaptive filter, which is primarily intended to suppress the self-interference signal.

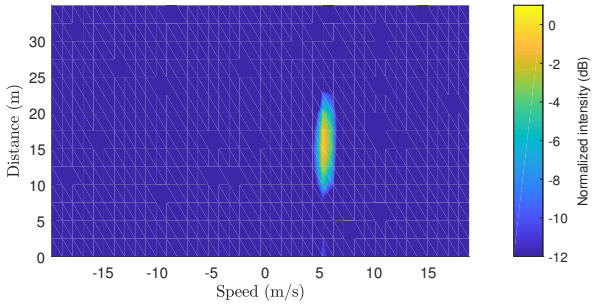

Fig. 4. Measured range-Doppler image produced from the offline-computed adaptive filter coefficient vector, which also provides 36 dB self-interference suppression.

IV. Experimental Result

Using a NI USRP, the proposed method is also evaluated by transmitting a 20 MHz OFDM communication signal. We also equipped the device with a customized electrical balance duplexer (EBD) [12], which operates at 1.74 GHz frequency band. The EBD limits the Tx channel power to 8 dBm and enables 39 dB analog SI rejection. The baseband I/Q stream is then recorded at 60 MHz, while a test reflector moves at 14 m from the evaluation setup. The digital SI cancellation is applied offline by a 15-tap adaptive filter implemented in Matlab™. Due to the theoretical range resolution of the test waveform ($R_{res} = 7.49\ m$), we skipped weight averaging step in (9), and applied the decimation to all of the coefficients separately for a 135 ms observation window. This allows rendering a 2D radar graph illustrated in Fig. 4, in which the target is detected nearly at the expected location.

V. Conclusion

In this paper, we proposed a method to integrate radar into an IBFD communication device. The represented approach adopts the weight vector of the adaptive FIR filter, which is the second step of SI cancellation, to also perform range and Doppler detection. Such multi-function adaptive filtering in the IBFD context, to our knowledge, has not been studied in the literature. We validated the radar capability of the proposed solution by the standard IEEE 802.11ac waveform. The simulated multi-target scenario included four moving objects and a second party emitter, which concurrently transmits on the same band. Furthermore, using a proof of concept setup, we applied our technique to detect a moving object by a 20 MHz OFDM communication signal. The simulation and experimental results suggest that the accuracy of the radar is sufficient to meet the requirements of a broad spectrum of radar-communication applications, namely body/hand gesture detection, crowd clustering, and user tracking.

Various open challenges have to be tackled before prototyping. For example, the adaptation convergence time should be as rapid as the filter can track the fastest Doppler $f_{d,max}$, i.e., $T_c << 1/f_{d,max}$. This is practically dictated by the application, the frequency band and the bandwidth of the communication signal.

Acknowledgment

This work was funded by the European Union's Horizon 2020 under grant agreement no. 732174 (ORCA project).

References

[1] P. E. Howland, D. Maksimiuk, and G. Reitsma, "Fm radio based bistatic radar," *IEE Proceedings-Radar, Sonar and Navigation*, vol. 152, no. 3, pp. 107–115, 2005.

[2] R. Cardinali, F. Colone, C. Ferretti, and P. Lombardo, "Comparison of clutter and multipath cancellation techniques for passive radar," in *2007 IEEE Radar Conference*. IEEE, 2007, pp. 469–474.

[3] M. A. Attalah, T. Laroussi, F. Gini, and M. S. Greco, "Range-doppler fast block lms algorithm for a dvb-t-based passive bistatic radar," *Signal, Image and Video Processing*, vol. 13, no. 1, pp. 27–34, 2019.

[4] C. Sturm and W. Wiesbeck, "Waveform design and signal processing aspects for fusion of wireless communications and radar sensing," *Proceedings of the IEEE*, vol. 99, no. 7, pp. 1236–1259, 2011.

[5] P. Kumari, J. Choi, N. González-Prelcic, and R. W. Heath, "Ieee 802.11 ad-based radar: An approach to joint vehicular communication-radar system," *IEEE Transactions on Vehicular Technology*, vol. 67, no. 4, pp. 3012–3027, 2017.

[6] C. Sturm, T. Zwick, and W. Wiesbeck, "An ofdm system concept for joint radar and communications operations," in *VTC Spring 2009-IEEE 69th Vehicular Technology Conference*. IEEE, 2009, pp. 1–5.

[7] S. A. Hassani, A. Guevara, K. Parashar, A. Bourdoux, B. van Liempd, and S. Pollin, "An in-band full-duplex transceiver for simultaneous communication and environmental sensing," in *2018 52nd Asilomar Conference on Signals, Systems, and Computers*. IEEE, 2018, pp. 1389–1394.

[8] S. A. Hassani, K. Parashar, A. Bourdoux, B. van Liempd, and S. Pollin, "Doppler radar with in-band full duplex radios," in *IEEE INFOCOM 2019-IEEE Conference on Computer Communications*. IEEE, 2019, pp. 1945–1953.

[9] S. A. Hassani, V. Lampu, K. Parashar, L. Anttila, A. Bourdoux, B. v. Liempd, M. Valkama, F. Horlin, and S. Pollin, "In-band full-duplex radar-communication system," *IEEE Systems Journal*, 2020.

[10] A. Goldsmith, *Wireless communications*. Cambridge university press, 2005.

[11] B. Kovačević, Z. Banjac, and M. Milosavljević, *Adaptive digital filters*. Springer Science & Business Media, 2013.

[12] B. van Liempd, B. Hershberg, S. Ariumi, K. Raczkowski, K.-F. Bink, U. Karthaus, E. Martens, P. Wambacq, and J. Craninckx, "A+ 70-dbm iip3 electrical-balance duplexer for highly integrated tunable front-ends," *IEEE Transactions on Microwave Theory and Techniques*, vol. 64, no. 12, pp. 4274–4286, 2016.